

Impact of an Aortic Valve Implant on Body Surface UWB Propagation: A Preliminary Study

Wen-Bin Yang, Kamran Sayrafian-Pour, John
Hagedorn, Judith Terrill

Information Technology Laboratory
National Institute of Standards and Technology
Gaithersburg, Maryland, USA
{wyang, ksayrafian, hagedorn, judith.terril}@nist.gov

Kamya Yekeh Yazdandoost, Attaphongse
Taparugssanagorn, Matti Hämäläinen, Jari Iinatti

Center for Wireless Communications
University of Oulu, Finland
yazdandoost@ieee.org, attaphongset@gmail.com,
{matti.hamalainen, jari.iinatti}@ee.oulu.fi

Abstract — Efficient transceiver design in body area networks requires in-depth understanding of the propagation channel which in this case involves the human body. Several studies have been done to characterize RF propagation on the body surface and determine the parameters of an appropriate model. However, the possible effect of an already existing medical implant on body surface propagation has not been considered until during a recent measurement experiment. There it was discovered that an aortic implant may have an impact on Ultra Wide-Band (UWB) propagation between wearable nodes that are in the vicinity of the implant location. In this paper, we use a 3D immersive visualization environment to study and observe the impact of an aortic implant on body surface propagation. Specifically, we focus on the UWB impulse response of the channel between nodes located around the upper body. The difference in the obtained impulse responses (for scenarios with and without the implant) both in measurement and simulation points to the possible impact that such medical implants could have on body surface RF propagation.

Keywords – Body Area Networks; Ultra-WideBand (UWB); Immersive visualization system; Aortic Valve Implant

I. INTRODUCTION

Recent advances in microelectronics indicate that the technology to achieve ultra-small and ultra low power wearable and implantable devices is mostly available. Communication protocol between such radio-enabled devices constitutes a Body Area Network (BAN). Although, there are still numerous challenges in vast commercialization of such products, BAN is poised to be a promising interdisciplinary technology with novel uses in pervasive health information technology. For example, RF-enabled wearable sensor nodes offer an attractive set of applications, among which we can point to electrocardiogram (ECG) and various other medical monitoring applications such as temperature, respiration, heart rate, blood pressure and pH [4].

Due to the medical nature of these applications, successful adoption of this technology heavily depends on the existence of a global standard for its radio communication. Although factors such as interference and co-existence with other wireless technologies are extremely important in the choice for BAN operating frequency, worldwide availability (i.e.

partially) and also the opportunity to have small-sized antennas make UWB a favorable candidate for wearable BAN applications. Understanding the propagation channel which in this case involves the human body is a major requirement in order to design efficient BAN transceivers. For the case of wearable sensors, physical channel measurements have been the focus of several research studies in recent years. The results of these studies specify the parameters of an appropriate statistical channel model [8, 9] for wearable nodes. However, none of these studies consider the possible effect of an existing medical implant (such as a metallic heart valve) on body surface propagation.

During a recent measurement experiment at the Center for Wireless Communications at the University of Oulu, Finland, it was discovered that an aortic implant may have an impact on Ultra Wide-Band (UWB) propagation between wearable nodes that are in the vicinity of the implant location [5, 6]. The difference between impulse responses of two UWB nodes located around the upper body for the case of subjects with and without an aortic valve was significantly observable. This result prompted us to further study the possible impact of such medical implants on body surface propagation. To the best of our knowledge, this is the first study of its kind to consider this issue.

The complexity of the media and other practical issues in performing physical measurements (e.g. finding volunteers with implants and various safety issues) only allow for a very limited number of experiments. Therefore, we are using a sophisticated 3D immersive visualization platform to emulate the physical experiment and obtain further data that would have been normally very difficult or impossible. This innovative platform easily allows us to vary all relevant parameters (e.g. implant location, shape, size, material) and investigate the impact of each one of them on the channel response.

In the following sections, we briefly describe the results of the experiment and simulation and how they both point to the possible effect of the aortic implant on the observed channel impulse response. Here, we are only reporting preliminary results of this study. The authors plan to continue this work to

extensively investigate the impact of medical implants on body surface propagation. The rest of this paper is as follows. Section 2 will describe the measurement setup and its results. The immersive 3D platform that has been used for our simulations is discussed in Section 3. Then, description of the simulated scenarios and results are provided in Section 4. Finally concluding remarks and future plans are expressed in Section 5.

II. MEASUREMENT SETUP & RESULTS

The channel measurement system consisted of an HP Agilent¹ 8720ES Vector Network Analyzer (VNA), P200 BroadSpec™ antennas [10], 5-m long SUCOFLEX® RF cables with 7.96 dB loss and a control computer with Lab-VIEW™ 7 software. The VNA is operated in a transfer function measurement mode, where port 1 and port 2 are the transmitting and the receiving port, respectively, as seen in Figure 1. This corresponds to a S21 parameter measurement set-up, where the device under test is the radio channel. The BroadSpec™ antennas are azimuthally omni-directional with the antenna radiation patterns as shown in [12]. The sweep time of the network analyzer depends on the number of frequency points within the sweep band, being automatically adjusted by the VNA. The frequency band used in the measurements is from 3.1 GHz to 10 GHz covering almost the whole frequency band of the UWB mask allotted by the FCC (i.e. 3.1-10.6 GHz) [6]. Therefore, the bandwidth (B) of the probe signal is 6.9 GHz. The maximum number of frequency points per sweep M is 1601. This leads to a maximum detectable channel delay (τ_{max}) of 231 ns. The measurements were carried out in the frequency domain but transferred to the time domain at the VNA, which gives the impulse responses of the channel as outputs for further analysis.

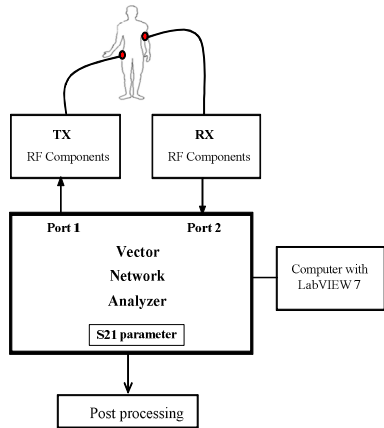


Figure 1. Measurement setup using the Vector Network Analyzer

The UWB channel measurement experiments were conducted in an anechoic chamber to minimize the effect of the environment when measuring the channel around the body. The measurements were taken at the chest level (around the body) as illustrated in Figure 2. The Rx antenna (the rectangle

in the figure) is fixed at the middle front of the torso and the Tx antenna (the circles in the figure) is placed at various positions at separations of about 10 cm. Further details about the experiments can be found in [5, 6].

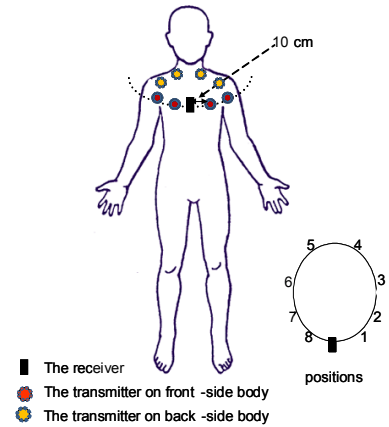


Figure 2. Antenna positions around the chest

The results were obtained for 3 men; one of them has a titanium alloy aortic valve implant made by Medtronic² as shown in Figure 3.



Figure 3. Medtronic Hall Aortic Heart Valve

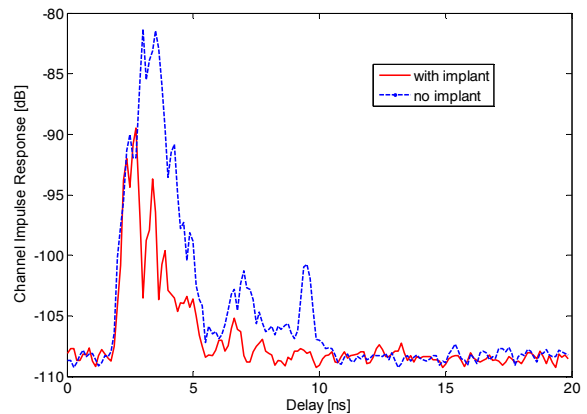


Figure 4. Average channel impulse response for position 2

¹ Identification of the Agilent VNA does not imply recommendation or endorsement by the National Institute of Standards and Technology.

² Medtronic Hall Aortic Heart Valve is a product of Medtronic Inc. Identification of this product does not imply recommendation or endorsement by the National Institute of Standards and Technology.

One hundred realizations of the measured channel impulse responses were averaged for each position. Figure 4 shows that the average channel impulse response (for position 2) of the subject with an aortic implant in comparison with the subjects with no implants. As observed, there is a clear difference between the magnitudes of the channel responses in these two scenarios. In this paper, results for the other positions have been omitted for brevity. Although, the valve implant is located inside the heart, the metallic material used in its construction (i.e. titanium) seems to be making an impact on RF propagation along the chest surface. To better understand this impact, we have decided to emulate this experiment in a 3D virtual reality platform and see if similar results are observed. This simulation platform is briefly described in the next section.

III. A 3D IMMERSIVE SYSTEM FOR WEARABLE & IMPLANTABLE MEDICAL SENSORS

Figure 5 shows the block diagram of our simulation environment. As observed, the main components of this system include: a three-dimensional human body model, the propagation engine which is a three-dimensional full-wave electromagnetic field simulator (i.e. HFSS³) and the 3D immersive & visualization platform. The 3D human body model includes frequency dependent dielectric properties of 300+ parts in a male human body. These properties are also user-definable if custom changes or modifications are desired. The human body model has a resolution of 2 mm. The HFSS propagation engine enables us to compute a variety of different electromagnetic quantities such as the magnitude of electric and magnetic fields Poynting vectors, and Specific Absorption Rate (SAR).

The 3D immersive platform as shown in Figure 6 includes several components: three orthogonal screens that provide the visual display, the motion tracked stereoscopic glasses, and the hand-held motion tracked input device. The screens are large projection video displays that are placed edge-to-edge in a corner configuration. These three screens are used to display a single three-dimensional stereo scene. The scene is updated based on the position of the user as determined by the motion tracker. This allows the system to present to the user a 3D virtual world within which the user can move and interact with the virtual objects. The main interaction device is a hand-held three button motion-tracked wand with a joystick. A user in this virtual environment can look at data representations at any scale and position, move through data, change orientation, and control the elements of the virtual world using a variety of interaction techniques including measurement and analysis [1]. All of these capabilities are extremely useful when studying RF propagation for wearable or implantable medical sensors [7, 11].

Input parameters to the 3D simulation system include: a wearable/implantable antenna and all its relevant attributes (i.e.

³ HFSS is registered trademark of ANSYS Inc. The HFSS has been used in this research to foster understanding. Such identification does not imply recommendation or endorsement by the National Institute of Standards and Technology, nor does it imply that this product is necessarily the best available for the purpose.

its characteristics, exact position on the body and its orientation), operating frequency, transmit power, resolution, range and the choice of the desired output parameter. Resolution of 4 mm has been selected to run the simulations in this study.

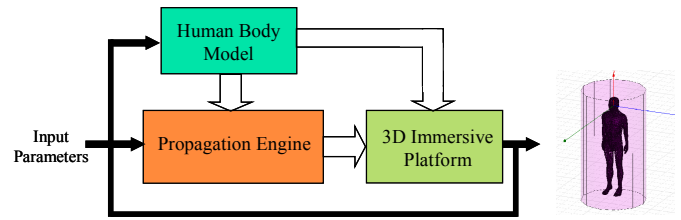


Figure 5. System block diagram

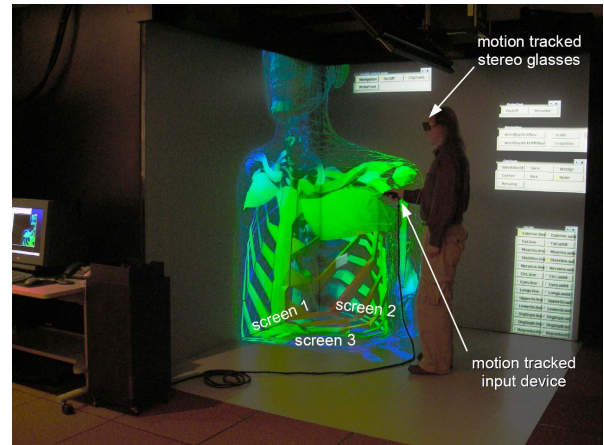


Figure 6. A User in the NIST Immersive Visualization Environment

For UWB simulations, we have used the loop antenna shown in Fig. 7. This antenna has an operating frequency range of 3.1-5.1 GHz and its size is 29.25×38.5×1 mm. It is printed on a side of FR4 substrate with dielectric constant of $\epsilon_r = 4.4$ and loss tangent of $\tan\theta = 0.02$. To avoid performance degradations such as pattern distortion, power absorption and central frequency shift, the influence of human body has been carefully accounted for in the design of this antenna. Figure 8 displays the VSWR (Voltage Standing Wave Ratio) of the antenna in proximity to human body. Detailed study of the characteristics of this antenna in free space and also in close proximity to human body has been provided in [2, 3].

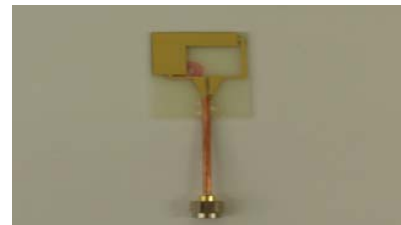


Figure 7. The UWB Loop Antenna

We have also simulated the aortic valve implant based on the size (and approximate shape) information provided in the Medtronic product specification data sheet [12]. Figure 9

displays the simulated aortic implant in the 3D immersive platform. Attention was also given to the proper location of the valve with respect to the body surface.

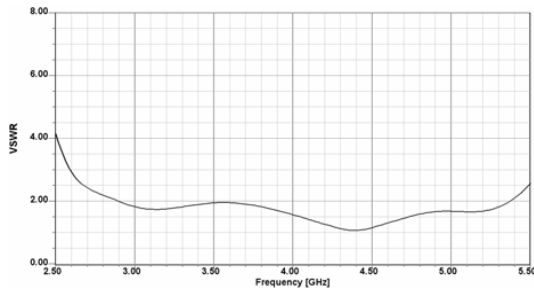


Figure 8. The UWB antenna VSWR in proximity to the body surface

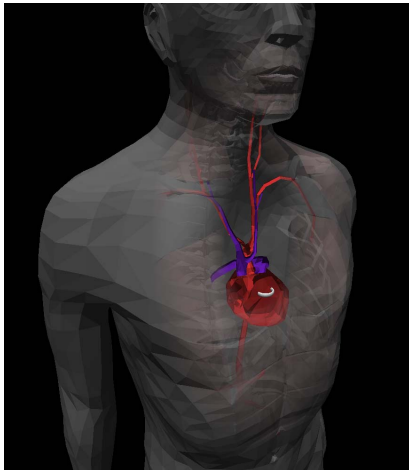


Figure 9. Simulation of the aortic heart valve in the NIST Immersive Visualization Environment

IV. SIMULATION SCENARIOS & RESULTS

Figure 10 displays the relative positions of the receivers and transmitters in our simulation. The circle indicates the cross-section of the chest around the upper body. The receiver positions are marked with red circles while the transmitter position is marked with a green box. The receiver locations have been chosen to mimic their corresponding positions in the experiment described in section 2 (i.e. positions 1 through 8). In all cases, the antenna was located about 12 mm away from the body surface to have the best performance. Also, although, the exact location of the aortic valve is approximately identifiable in our 3D system, in order to gain more insight, 2 different depths were chosen for the initial placement of the implant. Those were 32 mm and 80 mm below the body surface. This will lead to 3 different scenarios for our simulations: 1) no aortic valve, 2) with aortic valve at 32 mm below body surface and 3) with aortic valve at 80 mm below body surface.

For each receiver location, the frequency response of the channel was calculated across the UWB frequency range of 3.1 to 5.1 GHz with a step size of 40 MHz. Figure 11 displays the

frequency responses (i.e. S_{21}) corresponding to position ‘a’ for the 3 scenarios just mentioned. As observed, all channel responses are highly frequency dependent and not quite identical.

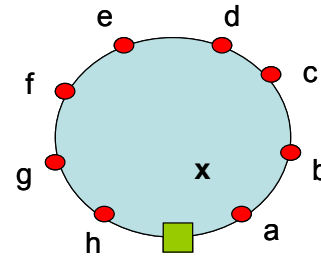


Figure 10. Transmitter and various receivers locations around the chest

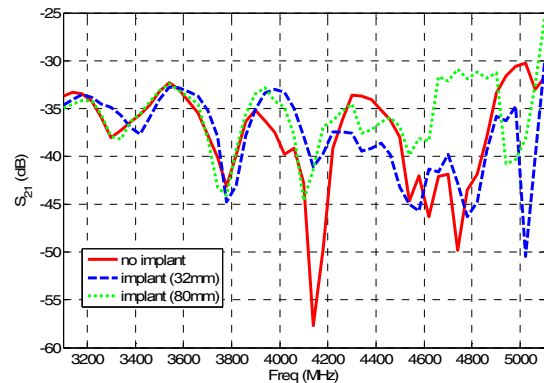


Figure 11. Frequency domain channel response for position ‘a’

Using IFFT (Inverse Fast Fourier Transform) with appropriate Kaiser filtering, we can obtain the temporal response of the channel. For example, Fig. 12 represents the time-domain impulse response of the channel for position ‘a’. Due to the close proximity of position ‘a’ to the transmitter, the 3 curves are very similar; however, more variation is observed when the implant is located closer to the body surface (i.e. the blue curve).

Figures 13, 14 show the corresponding frequency and time domain impulse responses for position ‘b’, respectively. The difference between the implant and no-implant cases is more pronounced compared to position ‘a’. This is especially visible for the case where the implant is 32 mm below the body surface. However, this difference is not as significant as the result obtained by the measurements (Figure 4). There are a few main factors that mostly contribute to this discrepancy; for example type of the antenna used, the covered UWB bandwidth, and exact whereabouts (i.e. location & orientation) of the transmitter and receivers as well as the aortic implant. The transmitter antenna and its gain pattern could greatly impact the results of both simulation and experiment. Keep in mind that the antenna used for the experiment was an off-the-shelf antenna, while the antenna used in the simulation has been optimized for BAN application. Also, in the experiment, the entire UWB band (i.e. 3.1-10 GHz) has been used; where only the lower portion (3.1-5.1 GHz) was used in the

simulation. Finally, the locations of the node on the chest have only been approximately matched.

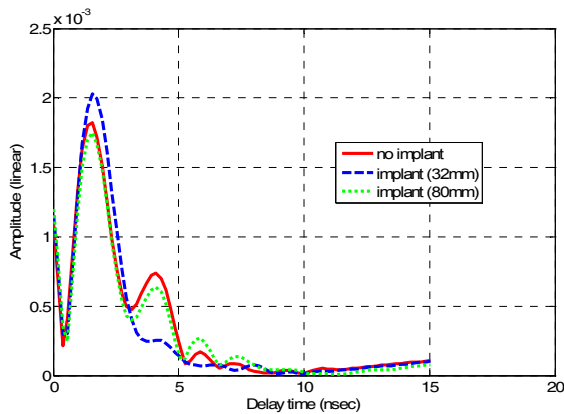


Figure 12. Channel impulse response for position 'a'

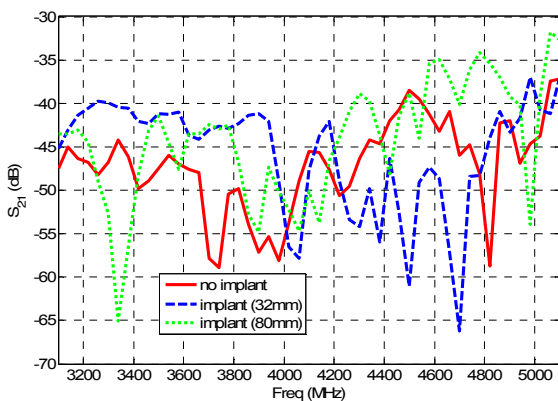


Figure 13. Frequency domain channel response for position 'b'

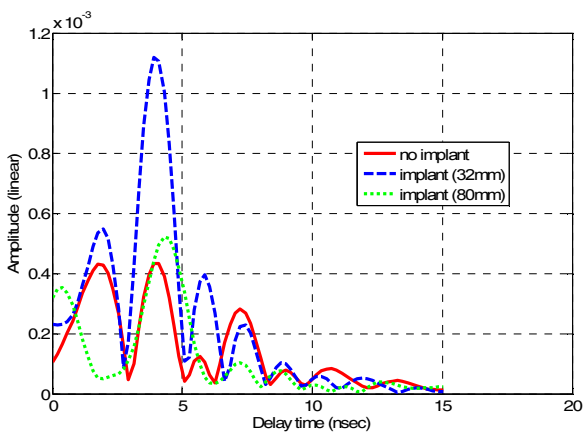


Figure 14. Channel impulse response for position 'c'

While the results of the simulation and experiment do not exactly match, the fact that they both exhibit an effect on UWB body surface propagation due to the presence of an aortic implant is clear. And, therefore, more in-depth study is required to investigate this issue. Results for positions 'c'

through 'h' also indicated some difference in the channel impulse response either in magnitude or delay. Those results, however, have been omitted for brevity.

V. CONCLUSION

Using a 3D virtual reality environment, we have studied the possible impact of an aortic valve implant on the body-surface propagation for wearable sensors. In particular, we looked at the impulse response when the transmitter/receivers were located around the upper body and in the vicinity of the implant. The results of both experiment and simulation point to the fact that the existence of the implant with titanium alloy material does indeed impact the magnitude of the channel impulse response. Since extensive physical experiment is very difficult to perform, the 3D immersive system proves to be a valuable scientific tool to investigate this issue in detail. The authors plan to continue this study by coordinating both experiments and simulations using the same set of parameters and scenarios.

REFERENCES

- [1] J. G. Hagedorn, J. P. Dunkers, S.G. Satterfield, A. P. Peskin, J. T. Kelso, J. E. Terrill, "Measurement tools for the immersive visualization environment: Steps toward the virtual laboratory", *Journal of research, NIST*, Vol. 112, No. 5, Sept.-Oct. 2007.
- [2] K. Y. Yazdandoost, R. Kohno, "Ultra Wideband L-loop antenna," *IEEE International Conference on Ultra-Wideband*, 2005.
- [3] K.Y. Yazdandoost, R.Kohno, "UWB Antenna for Wireless Body Area Network", *Proceedings of Asia-Pacific Microwave Conference 2006*.
- [4] G. Yang, "Body sensor networks", Springer-Verlag London Limited 2006, ISBN 1-84628-272-1.
- [5] A. Taparugssanagorn, C. Pomalaza-Raez, A. Isola, R. Tesi, M. Hämäläinen, J. Iinatti, "UWB Channel Modeling for Wireless Body Area Networks in Medical Applications", *Int. Symposium on Medical Info. and Communication Tech., ISMICT 2009*.
- [6] A. Taparugssanagorn, C. Pomalaza-Raez, A. Isola, R. Tesi, M. Hämäläinen, J. Iinatti: "UWB channel modeling for wireless body area networks in a hospital," *International. Journal of Ultra Wideband Communications and Systems (IJUWBCS)*, Vol. 1, No. 4, 2010, pp. 226 – 236.
- [7] K. Sayrafian-Pour, W. Yang, J. Hagedorn, J. Terrill, K. Y. Yazdandoost, "A Statistical Path Loss Model for Medical Implant Communication Channels", *IEEE PIMRC 2009*.
- [8] A. Fort, J. Ryckaert, C. Desset, P. Doncker, P. Wambacq, L. V. Biesen, "Ultra-Wideband Channel Model for Communication Around the Human Body", *IEEE Journal on Selected Areas in Communications*, Vol. 24, No. 4, April 2006.
- [9] T. Zasowski, F. Althaus, M. Stager, A. Wittneben, G. Troster, "UWB for Noninvasive Wireless Body Area Networks: Channel Measurements and Results", *Proc. IEEE Conf. Ultra Wideband Syst. Technol.*, Nov. 2003, pp. 285-289.
- [10] TimeDomain Corporation, P210 Integratable Module Data Sheet, 320-0095 Rev B, TimeDomain Corp., Huntsville, AL.
- [11] W. Yang, K. Sayrafian-Pour, J. Hagedorn, J. Terrill, K. Y. Yazdandoost, "Simulation Study of Body Surface RF Propagation for UWB Medical Sensors", *2nd International Symposium on Applied Sciences in Biomedical and Communication Technologies, ISABEL 2009*, Nov. 24-27, 2009
- [12] Butchart EG, Hui-Hua L, Payne N, et al. Twenty years' experience with Medtronic Hall valve. *J.Thorac Cardiovasc Surg.* 2001; 121:1090-100